

Seismic characterization of dipping fractures in transversely isotropic background

Vladimir Grechka and Ilya Tsvankin*, Colorado School of Mines, Center for Wave Phenomena, Department of Geophysics, Golden, CO 80401-1887, USA

(V. Grechka currently is at Shell E&P, 3737 Bellaire Blvd., P.O.Box 481, Houston, TX 77001)

Summary

Although it is believed that natural fracture sets predominantly have near-vertical orientation, oblique stresses and other mechanisms may tilt fractures away from the vertical. Here, we examine an effective medium produced by a single system of obliquely dipping, rotationally invariant fractures embedded in a VTI (transversely isotropic with a vertical symmetry axis) background rock. This model is monoclinic with a vertical symmetry plane that coincides with the dip plane of the fractures.

Multicomponent seismic data acquired over such a medium possess several distinct features that make it possible to estimate the fracture orientation. For example, the vertically propagating fast shear wave (and the fast converted PS-wave) is typically polarized in the direction of the fracture strike. In contrast, the polarization vector of the slow shear wave at vertical incidence does *not* lie in the horizontal plane – an unusual phenomenon that can be used to detect oblique fractures. The normal-moveout (NMO) ellipses of horizontal events are co-oriented with the dip and strike directions of the fractures, which provides an independent estimate of the fracture azimuth.

Both the fracture and background parameters can be obtained from multicomponent wide-azimuth data using the vertical velocities and NMO ellipses of P-waves and two split S-waves (pure shear modes can be replaced by PS-waves) reflected from horizontal interfaces. Numerical tests corroborate the accuracy and stability of the inversion algorithm based on the exact expressions for the vertical and NMO velocities.

Introduction

Characterization of naturally fractured reservoirs using seismic data is a topic of significant importance to both exploration and reservoir development. While most existing research in seismic fracture characterization is done for vertical fracture sets, there is growing evidence that obliquely dipping fractures are not uncommon. For example, Angerer et al. (2002) identified dipping fractures in the Emilio field (Adriatic Sea) and used the asymmetry of the traveltimes of mode-converted PS-waves to estimate the fracture parameters. Although the combination of fracture dip and background anisotropy (e.g., transverse isotropy) may create rather complicated, low-symmetry anisotropic models, Grechka and Tsvankin (2002a) showed that the inversion of seismic data for the fracture compliances and orientations actually becomes better posed if the fractures are rotated away from the vertical.

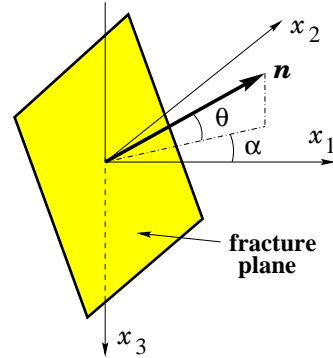


Fig. 1: Orientation of a fracture set is described by the dip θ and azimuth α of the vector \mathbf{n} orthogonal to the fracture plane. Since the background is azimuthally isotropic, we assume that the fracture strike is parallel to the x_2 -axis, and $\alpha = 0$.

Here, we study the effective medium produced by dipping, penny-shaped fractures in a VTI matrix – a model that may be quite typical for naturally fractured reservoirs. We describe seismic signatures for a wide range of fracture dips and devise a fracture-characterization procedure that operates with the kinematics of wide-azimuth P and S reflections.

Effective anisotropic medium

Consider a single set of parallel, dipping, rotationally invariant (penny-shaped) fractures embedded in a VTI background (Figure 1). According to the linear-slip theory (e.g., Schoenberg, 1980; Schoenberg and Sayers, 1995), the effective compliance matrix \mathbf{s} of a fractured medium can be found as the sum of the background compliance \mathbf{s}_b and the fracture compliance \mathbf{s}_f . For penny-shaped cracks, the matrix \mathbf{s}_f depends on just two compliances – normal (K_N) and tangential (K_T). If the fracture set is dipping, \mathbf{s}_f has to be rotated according to the so-called Bond transformation (e.g., Grechka et al., 2003). The stiffness matrix of the effective medium has the following form (the x_1 -axis points in the dip direction of the fractures):

$$\mathbf{c} \equiv \mathbf{s}^{-1} = \begin{pmatrix} c_{11} & c_{12} & c_{13} & 0 & c_{15} & 0 \\ c_{12} & c_{22} & c_{23} & 0 & c_{25} & 0 \\ c_{13} & c_{23} & c_{33} & 0 & c_{35} & 0 \\ 0 & 0 & 0 & c_{44} & 0 & c_{46} \\ c_{15} & c_{25} & c_{35} & 0 & c_{55} & 0 \\ 0 & 0 & 0 & c_{46} & 0 & c_{66} \end{pmatrix}. \quad (1)$$

The matrix \mathbf{c} describes a monoclinic medium with a vertical symmetry plane that coincides with the dip plane

Dipping fractures in TI background

$[x_1, x_3]$ of the fracture set. The effective medium becomes orthorhombic (this model was examined by Bakulin et al., 2000) when the fractures are vertical, and $c_{15} = c_{25} = c_{35} = c_{46} = 0$. The 13 elements of the effective stiffness matrix \mathbf{c} [equation (1)] depend on just eight independent quantities (five VTI background parameters, two fracture compliances, and fracture dip).

Analysis of seismic signatures

The exact expressions for the stiffness coefficients (1) are lengthy, but they can be simplified by assuming weak background anisotropy and small fracture weaknesses Δ_N and Δ_T defined as

$$\Delta_N \equiv \frac{K_N c_{11b}}{1 + K_N c_{11b}} \quad \text{and} \quad \Delta_T \equiv \frac{K_T c_{44b}}{1 + K_T c_{44b}}, \quad (2)$$

where c_{ijb} are the background stiffnesses. The weak-anisotropy approximations for the stiffness elements c_{ij} , linearized in Δ_N , Δ_T and the anisotropic parameters, help to derive explicit expressions for the seismic signatures analyzed below.

Polarizations and phase velocities for vertical propagation

As follows from the Christoffel equation, the polarization vector of one of the vertically traveling S-waves (S_{\parallel}) is parallel to the fracture strike. Both the P-wave and the second split S-wave (we denote it S_{\perp}) are polarized in the dip plane of the fractures, but their polarization vectors deviate from the vertical and horizontal directions, respectively. This deviation is caused entirely by the influence of the *obliquely dipping* fractures and depends on the angle θ between the fracture plane and the vertical (Figure 1).

The vertical phase velocity of the S_{\parallel} -wave in the weak-anisotropy approximation is

$$V_{S_{\parallel}} = V_{S0b} \left(1 - \frac{\Delta_T}{2} \sin^2 \theta \right), \quad (3)$$

where V_{S0b} is the vertical S-wave velocity in the VTI background. The linearized velocity of the S_{\perp} -wave at vertical incidence depends on both weaknesses and the squared ratio g_b of the S- and P-wave background velocities ($g_b \equiv V_{S0b}^2/V_{P0b}^2$):

$$V_{S_{\perp}} = V_{S0b} \left[1 - \frac{1}{4} (g_b \Delta_N + \Delta_T) + \frac{1}{4} (g_b \Delta_N - \Delta_T) \cos 4\theta \right]. \quad (4)$$

For the special case of vertical fractures ($\theta = 0^\circ$) equation (4) reduces to $V_{S_{\perp}}(\theta = 0) = V_{S0b}(1 - \Delta_T/2)$, so $V_{S_{\perp}} < V_{S_{\parallel}}$. Hence, for vertical fractures the shear-wave splitting coefficient at vertical incidence is controlled solely by the tangential compliance related to the crack density e as $\Delta_T \approx 2e$. For obliquely dipping fractures, however, the velocity of the wave S_{\perp} [equation (4)] and the splitting

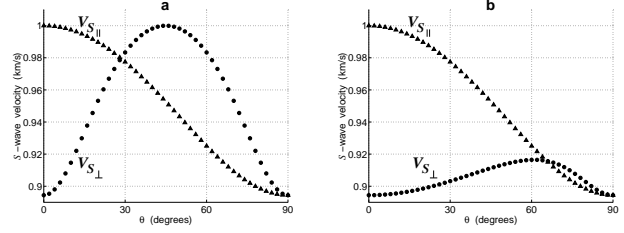


Fig. 2: Exact vertical phase velocities of the waves S_{\parallel} (triangles) and S_{\perp} (circles) for a fracture set tilted away from the vertical by the angle θ . The background parameters are $V_{P0b} = 2$ km/s, $V_{S0b} = 1$ km/s, $\epsilon_b = 0.3$, $\delta_b = 0.2$ and $\gamma_b = 0.4$. The fracture weaknesses are (a) $\Delta_T = 0.2$, $\Delta_N = 0$ (fluid-saturated fractures) and (b) $\Delta_T = 0.2$, $\Delta_N = 0.8$ (dry fractures).

coefficient also depend on the normal compliance Δ_N that varies with fluid saturation (Figure 2).

Analysis of equations (3) and (4) shows that if the fractures are dry (in this case $K_N = K_T$, and $\Delta_T \approx g_b \Delta_N$), then $V_{S_{\parallel}} \geq V_{S_{\perp}}$ for the whole range of fracture dips. For isolated fluid-filled fractures, the normal compliance Δ_N vanishes, and the inequality $V_{S_{\parallel}} \geq V_{S_{\perp}}$ is satisfied for $\theta < 30^\circ$. The above conclusions are confirmed by the results in Figure 2 obtained from the exact equations. The shear-wave velocities in Figure 2 are computed for a moderately anisotropic VTI background and a substantial value of the crack density $e \approx \Delta_T/2 = 0.1$. For fluid-filled fractures $V_{S_{\parallel}}$ is indeed greater than $V_{S_{\perp}}$ until θ reaches values close to 30° (Figure 2a). The weak-anisotropy prediction that for dry fractures $V_{S_{\parallel}} > V_{S_{\perp}}$ holds for angles $\theta < 65^\circ$ (Figure 2b). Therefore, unless the fractures deviate from the vertical by more than 30° , the fast shear wave at vertical incidence is polarized parallel to the fracture strike.

Pure-mode NMO velocities from a horizontal reflector

To estimate the VTI background parameters and fracture weaknesses, the velocities and polarization directions of the vertically propagating waves can be combined with the normal-moveout (NMO) ellipses of P- and S-waves from a horizontal interface. Since the fracture dip plane represents a vertical symmetry plane of the model, the axes of all NMO ellipses should be parallel to the dip and strike directions of the fracture set. The linearized expressions for the NMO ellipses based on the formalism of Grechka et al. (1999) show that the azimuthal variation of the P-wave NMO velocity [i.e., the difference χ_P between the velocities in the dip ($V_{\text{nmo},P}^{\text{dip}}$) and strike ($V_{\text{nmo},P}^{\text{str}}$) directions] is independent of the background Thomsen parameters ϵ_b , δ_b , and γ_b :

$$\chi_P = V_{\text{nmo},P}^{\text{dip}} - V_{\text{nmo},P}^{\text{str}} = 2g_b V_{P0b} \cos^2 \theta [2\Delta_T - \Delta_N(1 + g_b) - 3(\Delta_T - g_b \Delta_N) \cos 2\theta]. \quad (5)$$

Also, it is possible to combine the dip and strike components of the shear-wave NMO ellipses in such a way that the result depends just on the fracture weaknesses and

Dipping fractures in TI background

background velocities:

$$\tilde{\chi}_S = V_{\text{nmo},S_{\parallel}}^{\text{dip}} - V_{\text{nmo},S_{\perp}}^{\text{str}} = V_{S0b} \sin^2 \theta [g_b \Delta_N - \frac{\Delta_T}{2} + (\Delta_T - g_b \Delta_N) \cos 2\theta], \quad (6)$$

$$\hat{\chi}_S = V_{\text{nmo},S_{\perp}}^{\text{dip}} - V_{\text{nmo},S_{\parallel}}^{\text{str}} = V_{S0b} [-\Delta_T - g_b \Delta_N + 7(\Delta_T - g_b \Delta_N) \cos 4\theta]. \quad (7)$$

According to equation (5), the semi-major axis of the P -wave NMO ellipse points in the strike direction if the fractures do not strongly deviate from the vertical. Indeed, χ_P is negative for dry fractures ($\Delta_T \approx g_b \Delta_N$), while for fluid-filled fractures ($\Delta_N = 0$) $\chi_P < 0$ if $\theta < 24^\circ$.

The vertical velocities and the parameters χ_P , $\tilde{\chi}_S$, and $\hat{\chi}_S$ yield six equations which can be solved for five unknowns: the velocities V_{P0b} and V_{S0b} , the weaknesses Δ_N and Δ_T , and the fracture angle θ . The background coefficients ϵ_b , δ_b , and γ_b can then be estimated from the semi-axes of the NMO ellipses of P-waves and one of the S-waves. Below we verify the stability of this parameter-estimation scheme using exact expressions not limited to weak anisotropy.

Fracture characterization

The fast and slow shear waves at small and moderate incidence angles can be separated using Alford rotation. For the model at hand, the polarization vector of the fast S-wave at vertical incidence typically points in the direction of the fracture strike; the fracture azimuth can also be estimated from the NMO ellipses of horizontal events.

If shear waves are not excited, they can be replaced in polarization analysis by mode-converted PS-waves. Also, the reflection traveltimes of the waves S_{\parallel} and S_{\perp} can be obtained from 3-D multiazimuth P and PS (PS_{\parallel} and PS_{\perp}) reflection data using the methodology of Grechka and Tsavankin (2002b). The absence of the horizontal symmetry plane makes converted-wave reflection traveltimes asymmetric with respect to zero offset, even if the reflector is horizontal (Figure 3). The moveout asymmetry of mode conversions (that was used in fracture characterization by Angerer et al., 2002) does not prevent the algorithm of Grechka and Tsavankin (2002b) from obtaining the pure S-wave traveltimes, which are symmetric (i.e., reciprocal with respect to the source and receiver positions) in CMP geometry.

The pure-mode NMO ellipses (Figure 4) can then be reconstructed by means of 3-D (azimuthal) velocity analysis. After obtaining the “effective” NMO ellipses for the reflections from the top and bottom of the fractured layer, one can compute the interval NMO ellipses using the generalized Dix equation (Grechka et al., 1999). To constrain both the fracture and background parameters, the NMO ellipses of the P-, S_{\parallel} -, and S_{\perp} -waves have to be supplemented with the vertical velocities, which are assumed to be measured in a borehole.

The results in Figure 5 are obtained by applying nonlin-

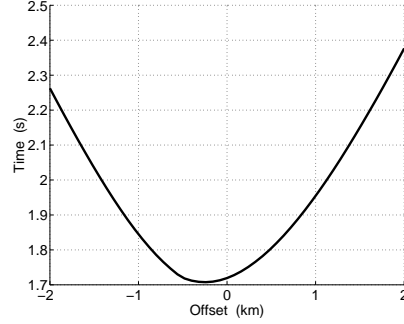


Fig. 3: Traveltime of the converted PS_{\perp} -wave computed in the fracture dip direction for $\theta = 25^\circ$. The reflector is horizontal at a depth of 1 km. The background parameters and fracture weaknesses are $V_{P0b} = 2.0$ km/s, $V_{S0b} = 0.9$ km/s, $\epsilon_b = 0.15$, $\delta_b = 0.05$, $\gamma_b = 0.05$, $\Delta_T = 0.1$, and $\Delta_N = 0.4$ (corresponds to dry fractures).

ear inversion based on the exact equations for the vertical velocities and the semi-axes of the NMO ellipses of the three pure-mode reflections. To verify the stability of the inversion algorithm, we added Gaussian noise with the standard deviations of 0.5% and 2% to the vertical and NMO velocities, respectively. The inversion was repeated 100 times for different realizations of the noise to find the standard deviation of each parameter. The confidence intervals for the background anisotropic coefficients and the tangential weakness Δ_T are close to 0.02, which indicates that the inversion is sufficiently stable. For the normal weakness Δ_N , however, the interval is more broad (it reaches 0.06) because the sensitivity of the velocities to Δ_N is relatively low. The confidence intervals for the vertical background velocities V_{P0b} , V_{S0b} and the fracture angle θ (not shown in Figure 5) are 2.8%, 0.5% and 3.6%, respectively. Similar inversion results but with smaller error bars were obtained for fluid-filled fractures (Figure 6).

Discussion and conclusions

We discussed the properties of the effective anisotropic medium formed by obliquely dipping, penny-shaped fractures embedded in a VTI background. If the angle between the fracture plane and the vertical does not exceed 25 – 30° , some seismic signatures resemble those for vertical fractures. In particular, both the polarization vector of the vertically propagating fast S-wave and the semi-major axis of the P-wave NMO ellipse for horizontal reflectors are parallel to the fracture strike.

However, for obliquely dipping fractures the P-wave and the slow S-wave at vertical incidence are *not* polarized in the vertical and horizontal directions, respectively. Their polarization vectors are rotated within the dip plane of the fractures around the fracture strike by an angle dependent on the fracture dip and weaknesses. Therefore, a substantial vertical displacement component of the slow S-wave (or a horizontal component of the P-wave) at near-vertical incidence serves as a strong indicator of oblique fractures. Also, as the fractures deviate from the vertical,

Dipping fractures in TI background

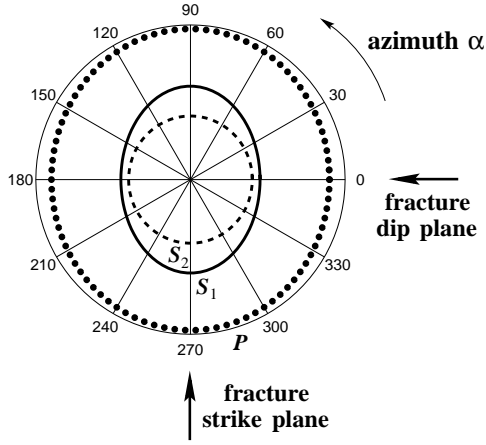


Fig. 4: Pure-mode NMO ellipses in a horizontal fractured layer with the parameters given in Figure 3. The fast shear mode S_1 is the S_{\parallel} -wave, and the slow mode S_2 is the S_{\perp} -wave. The thin outer circle corresponds to a velocity of 2 km/s.

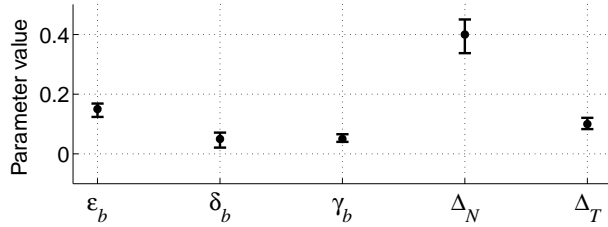


Fig. 5: Fracture and background parameters of the model from Figure 3 obtained by nonlinear inversion of the vertical velocities and the NMO ellipses of the waves P, S_{\parallel} , and S_{\perp} . The dots mark the correct values; the error bars correspond to the 95% confidence intervals.

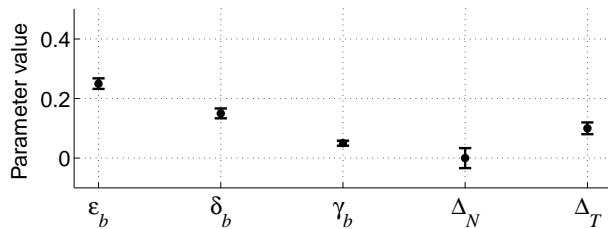


Fig. 6: Same as Figure 5 but for fluid-filled fractures ($\Delta_N = 0$). The 95% confidence intervals for the parameters V_{P0b} , V_{S0b} , and θ (not shown) are 2.0%, 0.5%, and 1.7°, respectively.

the velocity of the slow S-wave and the shear-wave splitting coefficient at vertical incidence become sensitive to fracture infill (i.e., to fluid saturation).

Although the effective medium is monoclinic, it is described by the fracture azimuth and just eight (rather than 13) independent quantities: the VTI background parameters V_{P0b} , V_{S0b} , ϵ_b , δ_b , and γ_b , the normal and tangential fracture weaknesses Δ_N and Δ_T , and the fracture deviation angle θ . Using nonlinear inversion based on the exact equations, we showed that all eight parameters can be estimated from the vertical velocities and NMO ellipses of P-waves and split shear waves S_{\parallel} and S_{\perp} . The normal weakness Δ_N is obtained with lower accuracy than the other parameters, but the overall performance of the inversion algorithm is quite satisfactory. The method of Grechka and Tsvankin (2002b) can be applied prior to the parameter estimation to replace the pure shear modes in the fracture-characterization procedure by the split converted (PS) waves.

The model treated here includes a single set of fractures, but the results of Grechka and Tsvankin (2002a) indicate that it may be possible to invert seismic data for the parameters of up to *four* dipping, rotationally invariant fracture sets in a VTI background.

References

- Angerer, E., Horne, S. A., Gaiser, J. E., Walters, R., Bagala, S., and Vetri, L., 2002, Characterization of dipping fractures using PS mode-converted data: 72nd Ann. Internat. Mtg., Soc. Expl. Geophys., Expanded Abstracts, 1010–1013.
- Bakulin, A., Grechka, V., and Tsvankin, I., 2000, Estimation of fracture parameters from reflection seismic data – Part II: Fractured models with orthorhombic symmetry: *Geophysics*, **65**, 1803–1817.
- Grechka, V., and Tsvankin, I., 2002a, Feasibility of seismic characterization of multiple fracture sets: 72nd Ann. Internat. Mtg., Soc. Expl. Geophys., Expanded Abstracts, 1646–1649.
- Grechka, V., and Tsvankin, I., 2002b, PP+PS=SS: *Geophysics*, **67**, 1961–1971.
- Grechka, V., Bakulin, A., and Tsvankin, I., 2003, Seismic characterization of vertical fractures described as general linear-slip interfaces: *Geophys. Prosp.*, **51**, 117–130.
- Grechka V., Tsvankin, I., and Cohen, J.K., 1999, Generalized Dix equation and analytic treatment of normal-moveout velocity for anisotropic media: *Geophys. Prosp.*, **47**, 117–148.
- Schoenberg, M., 1980, Elastic wave behavior across linear slip interfaces: *J. Acoust. Soc. Am.*, **68**, 1516–1521.
- Schoenberg, M., and Sayers, C., 1995, Seismic anisotropy of fractured rock: *Geophysics*, **60**, 204–211.